No.332 (#41 – 47)

41. ATOMS: ALMA three-millimeter observations of massive star-forming regions - II. Compact objects in ACA observations and star formation scaling relations

42. The Dynamic Proto-atmospheres around Low-mass Planets with Eccentric Orbits

43. Implementation of stellar heating feedback in simulations of star cluster formation: effects on the initial mass function

44. Ejection of close-in super-Earths around low-mass stars in the giant impact stage

45. Magnetohydrodynamic Accretion-Ejection: Jets Launched by a Nonisotropic Accretion-disk Dynamo. I. Validation and Application of Selected Dynamo Tensorial Components

46. Magnetohydrodynamic Accretion-Ejection: Jets Launched by a Nonisotropic Accretion-disk Dynamo. II. A Dynamo Tensor Defined by the Disk Coriolis Number

47. The magnetic obliquity of accreting T Tauri stars

ATOMS: ALMA three-millimeter observations of massive star-forming regions - II. Compact objects in ACA observations and star formation scaling relations

Show affiliations | Show all authors

Liu, Tie; Evans, Neal J.; Kim, Kee-Tae; Goldsmith, Paul F.; Liu, Sheng-Yuan; Zhang, Qizhou; Tatematsu, Ken'ichi; Wang, Ke; Juvela, Mika; Bronfman, Leonardo; Cunningham, Maria R.; Garay, Guido; Hirota, Tomoya; Lee, Jeong-Eun; Kang, Sung-Ju; Li, Di; Li, Pak-Shing; Mardones, Diego; Qin, Sheng-Li; Ristorcelli, Isabelle ; ...

We report studies of the relationships between the total bolometric luminosity (L_{bol} or L_{TIR}) and the molecular line luminosities of J = 1 - 0 transitions of $H^{13}CN$, $H^{13}CO^+$, HCN, and HCO^+ with data obtained from ACA observations in the 'ATOMS' survey of 146 active Galactic star-forming regions. The correlations between L_{bol} and molecular line luminosities L'_{mol} of the four transitions all appear to be approximately linear. Line emission of isotopologues shows as large scatters in L_{bol}- L'_{mol} relations as their main line emission. The log(L_{bol}/ L'_{mol}) for different molecular line tracers have similar distributions. The L_{bol}-to- L'_{mol} ratios do not change with galactocentric distances (R_{GC}) and clump masses (M_{clump}). The molecular line luminosity ratios (HCN-to-HCO^+, $H^{13}CN$-to-$H^{13}CO^+$, HCN-to-$H^{13}CN$, and HCO^+-to-$H^{13}CO^+$) all appear constant against L_{bol}, dust temperature (T_d), M_{clump}, and R_{GC}. Our studies suggest that both the main lines and isotopologue lines are good tracers of the total masses of dense gas in Galactic molecular clumps. The large optical depths of main lines do not affect the interpretation of the slopes in star formation relations. We find that the mean star formation efficiency (SFE) of massive Galactic clumps in the 'ATOMS' survey is reasonably consistent with other measures of the SFE for dense gas, even those using very different tracers or examining very different spatial scales.

https://ui.adsabs.harvard.edu/abs/2020MNRAS.496.2821L/abstract

ATOMS survey：銀河系の星形成領域146個

ACA観測
- 放射光度
- 分子輝線光度

主輝線と同位体分子種輝線の両方が、高密度ガス質量のよいトレーサーとなる。
➔
ATOMSサーベイより求めた平均星形成効率は、別の測定方法より得られた値と大体一致する。

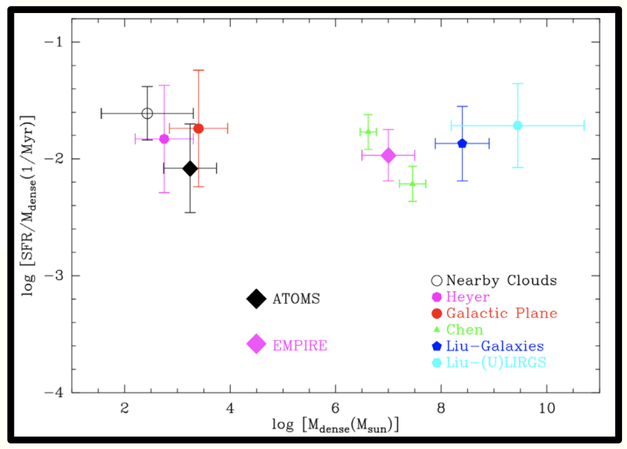

#41 M_{clump} vs L_{bol}, L_{mol}

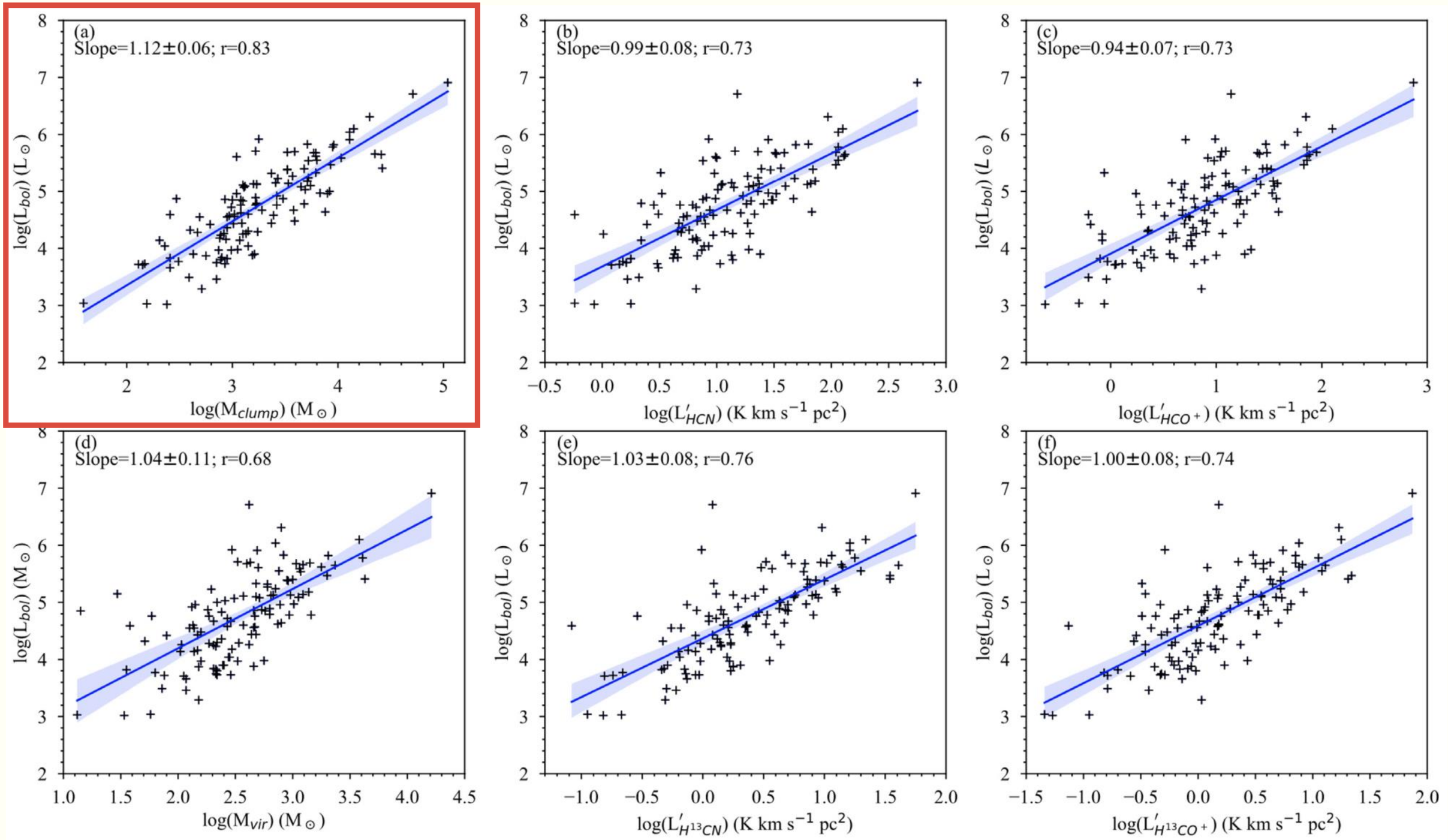

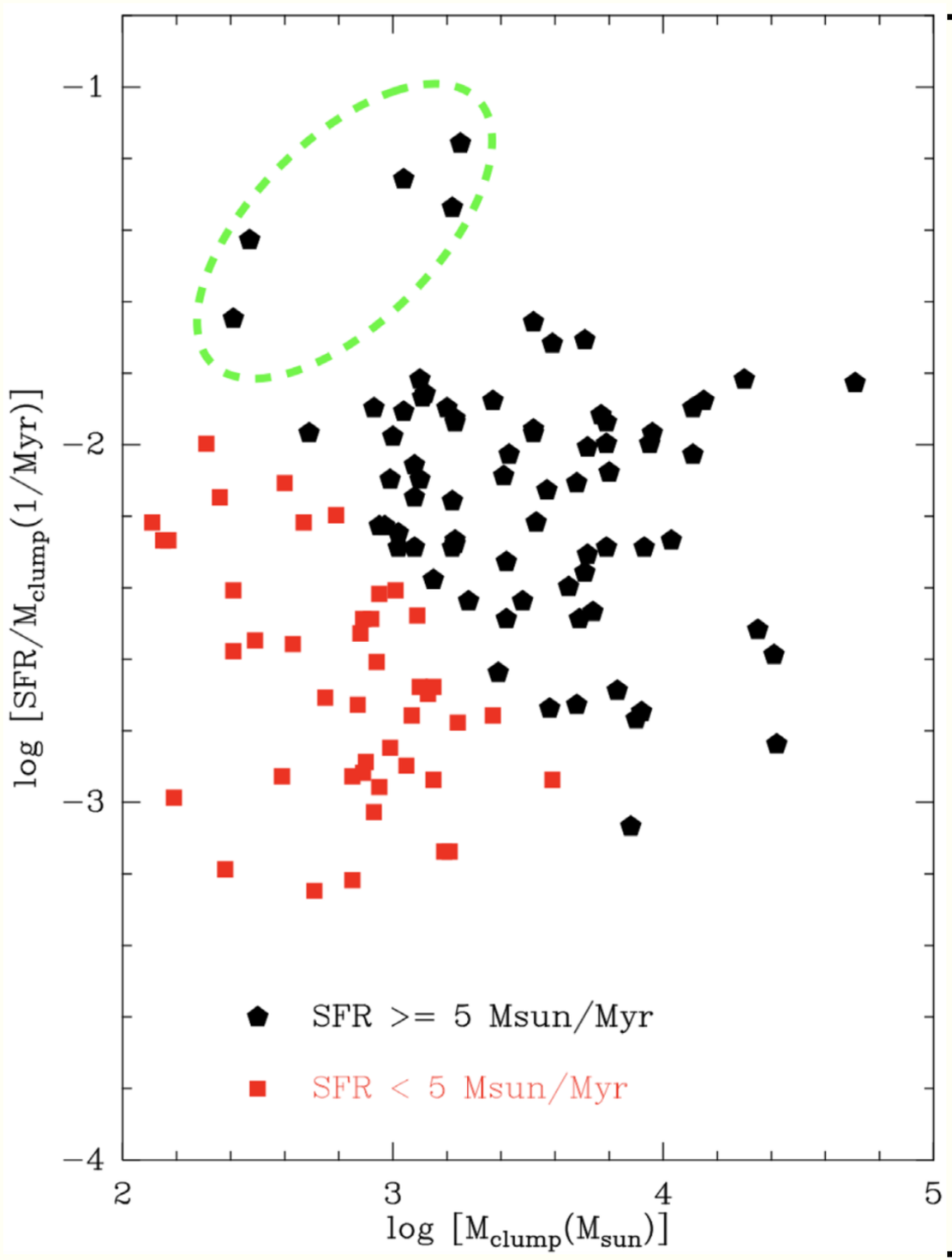

実際にはSFRはlocal IMFに応じて変わるが、他の観測結果と比較できるよう、先行研究と同じSFRを用いる。

$$\mathrm{SFR} = 1.49 \times 10^{-4} L_{\mathrm{bol}}(\mathrm{L}_\odot)\ \mathrm{M}_\odot\ \mathrm{Myr}^{-1}$$

SFE ≡ SFR/Mass

対数平均

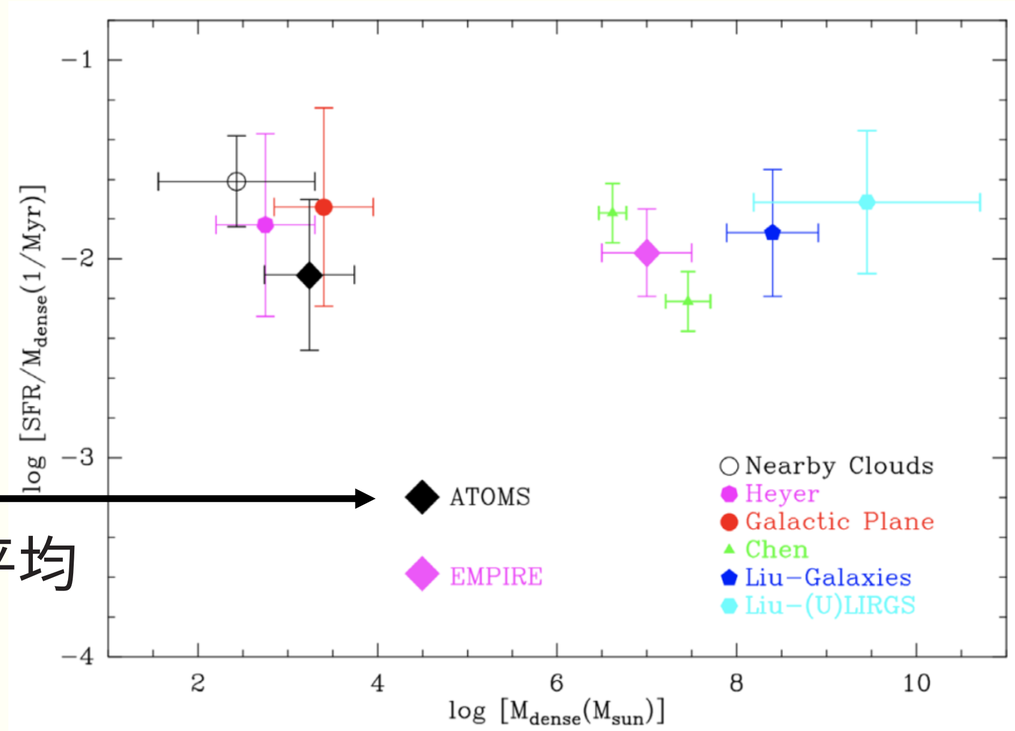

The Dynamic Proto-atmospheres around Low-mass Planets with Eccentric Orbits

Show affiliations

Mai, Chuhong; Desch, Steven J.; Kuiper, Rolf; Marleau, Gabriel-Dominique; Dullemond, Cornelis

Protoplanets are able to accrete primordial atmospheres when embedded in the gaseous protoplanetary disk. The formation and structure of the proto-atmosphere are subject to the planet-disk environment and orbital effects. In particular, when planets are on eccentric orbits, their velocities relative to the gas can exceed the sound speed. The planets generate atmosphere-stripping bow shocks. We investigate the proto-atmospheres on low-mass planets with eccentric orbits with radiation-hydrodynamics simulations. A 2D radiative model of the proto-atmosphere is established with tabulated opacities for the gas and dust. The solutions reveal large-scale gas recycling inside a bow shock structure. The atmospheres on eccentric planets are typically three to four orders of magnitude less massive than those on planets with circular orbits. Overall, however, a supersonic environment is favorable for planets to keep an early stable atmosphere, rather than harmful, due to the steady gas supply through the recycling flow. We also quantitatively explore how such atmospheres are affected by the planet's velocity relative to the gas, the planet mass, and the background gas density. Our time-dependent simulations track the orbital evolution of the proto-atmosphere with the planet-disk parameters changing throughout the orbit. Atmospheric properties show oscillatory patterns as the planet travels on an eccentric orbit, with a lag in phase. To sum up, low-mass eccentric planets can retain small proto-atmospheres despite the stripping effects of bow shocks. The atmospheres are always connected to and interacting with the disk gas. These findings provide important insights into the impacts of migration and scattering on planetary proto-atmospheres.

https://ui.adsabs.harvard.edu/abs/2020ApJ...899...54M/abstract

軌道離心率の大きい低質量惑星の原始大気

磁気流体シミュレーション

バウショックによる剥離効果にも関わらず、小さな原始大気を保持できる。

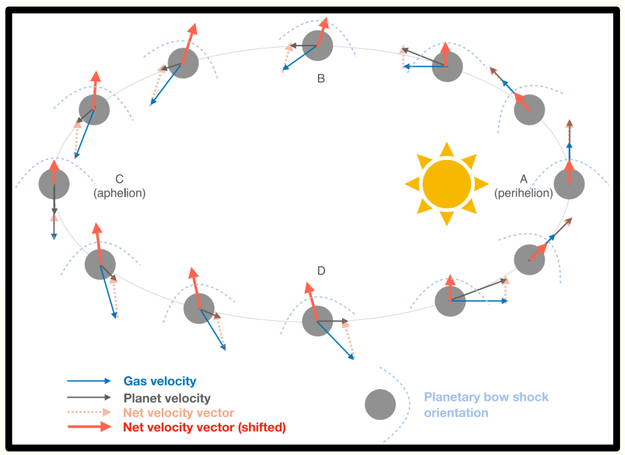

原始惑星 (protoplanets) は母体となった星雲が消散する前に形成し、星雲のガスから**原始大気**を獲得すると考えられている。

低質量惑星への星雲ガスの降着過程が計算されているが、これまでの研究では円軌道が仮定されていた。

見つかっている多くの太陽系外惑星は離心率の大きな軌道を持つ (e > 0.1)。そのような**偏心惑星 (eccentric planets)** は、星雲ガスと背景磁場を強くかき乱す。

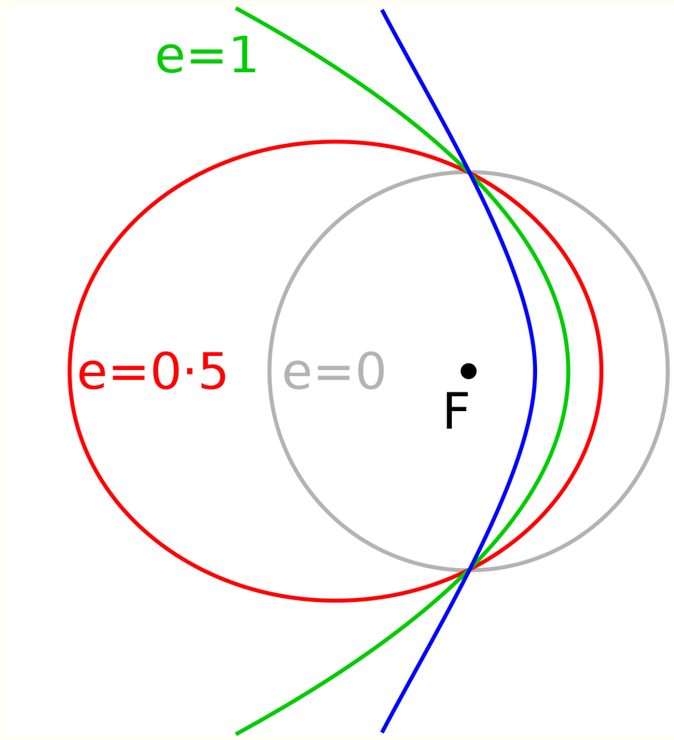

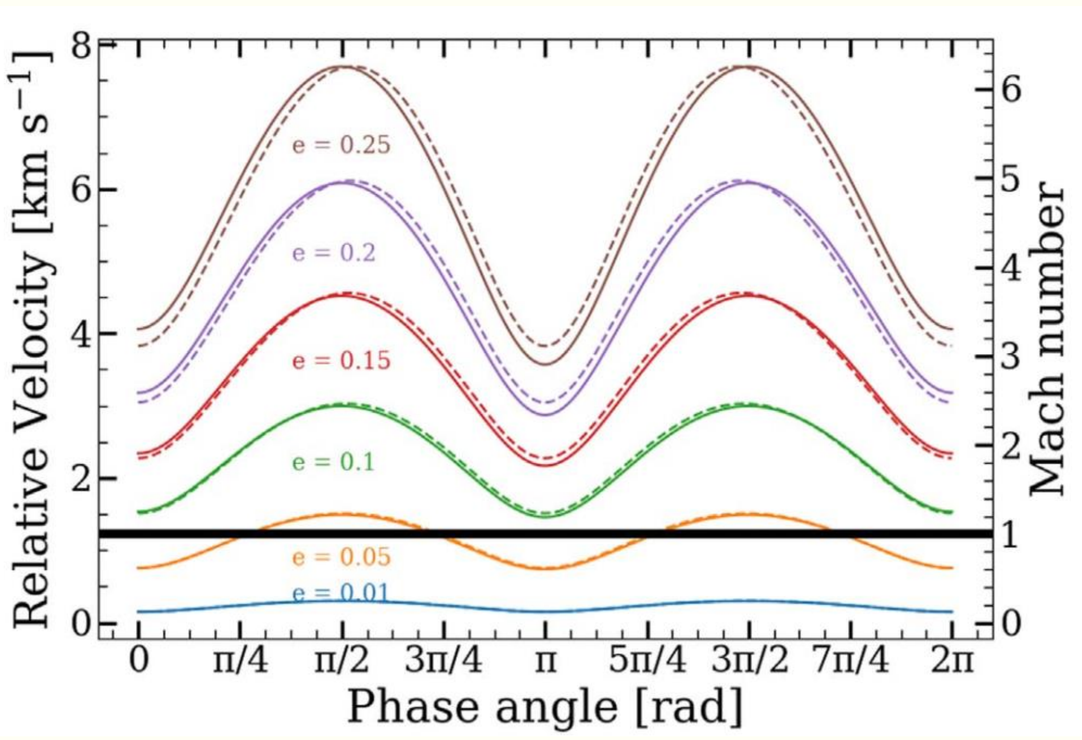

軌道離心率が**0.08以上**になると、全軌道中で惑星とガスの相対運動が**超音速**になる。

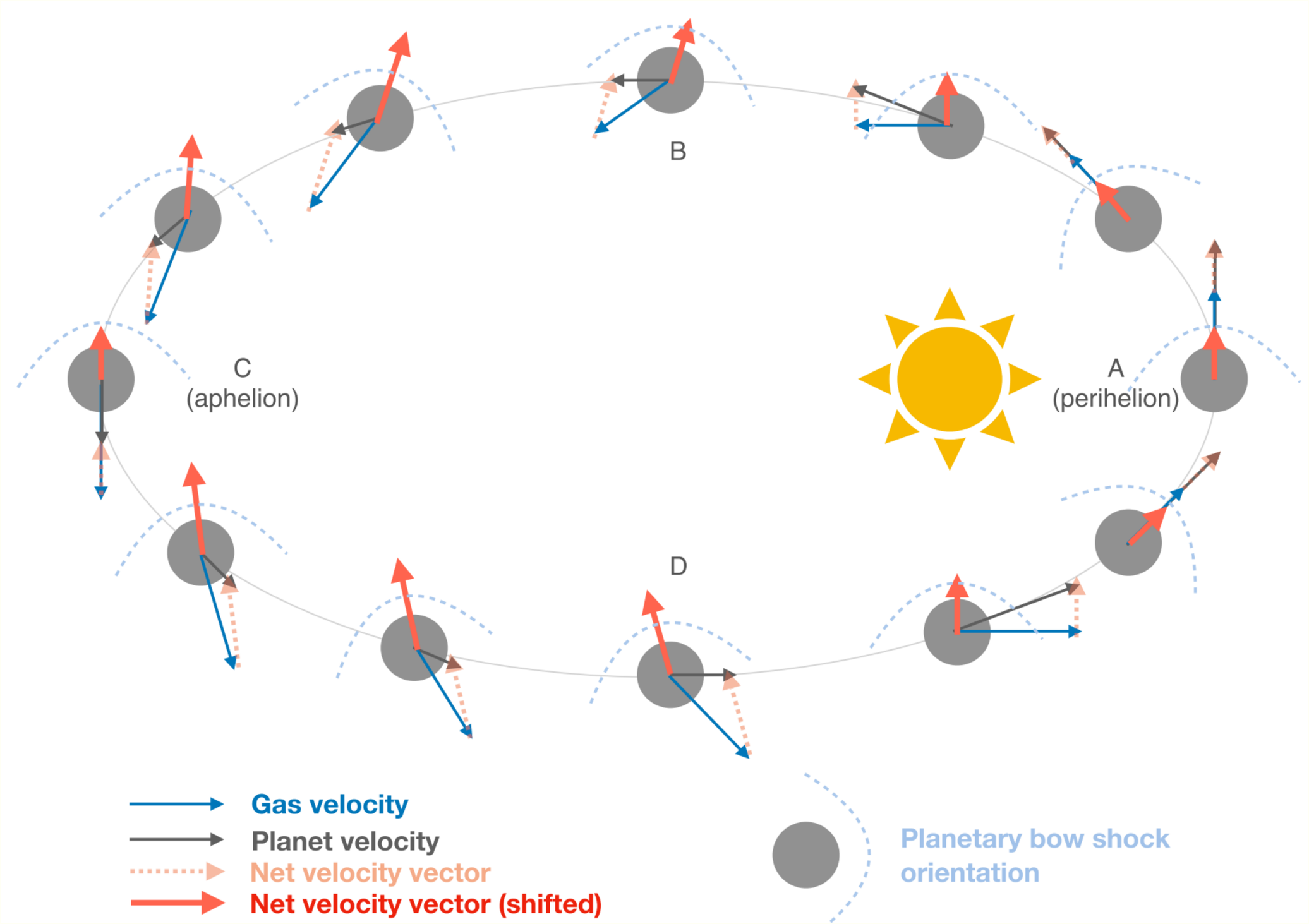
B
C
(aphelion)
A
(perihelion)
D
Gas velocity
Planet velocity
Net velocity vector
Net velocity vector (shifted)
Planetary bow shock
orientation

「偏心軌道 (e > 0.1) をとる惑星における原始大気形成」
➔「非粘性圧縮相同ガスを超音速で運動する重力的球体」でモデル化する

計算コード : PLUTO

- 輻射エネルギー輸送：Flux-Limited Diffusion (FLD)近似 (MAKEMAKE module)
- 状態方程式：円盤ガスは理想気体と仮定
- 運動する惑星を原点とした２次元軸対称球座標 (r, θ)：r = 1 to 1000 [R_{planet}]

境界条件 [Thun et al. 2016]

- 内側：惑星表面での反射境界
- 外側：ガス流入・流出

初期条件：Minimum Mass Solar Nebula (MMSN) model
[Weidenschilling 1977; Hayashi 1981; Thommes&Duncan 2006]

- 太陽から1 auの距離に位置する惑星 (M_{pl} = 1 $M_{earth,}$ R_{pl} = 1 R_{earth}) + 一様円盤ガス (T_{∞} = 300 K, ρ_{∞} = 10^{-9} g cm^{-3}) ... 数値はcanonical caseのもの
- Gas opacity data [Malygin et al. 2014]

#42　シミュレーションリスト

Table 1
List of Hydrodynamic Simulations

"Snapshot" Simulations

Name	v_∞ (km s^{-1})/$\mathcal{M}$	M_{pl} ($M_\oplus$)	ρ_∞ (g cm^{-3})	Comments
Canonical	**4.8/3.93**	**1.0**	**10^{-9}**	**The canonical case**
VEL3.2	3.2/2.64	1.0	10^{-9}	Sensitivity study on Mach number/ relative velocity
VEL3.7	3.7/3.02	1.0	10^{-9}	
VEL4.2	4.2/3.47	1.0	10^{-9}	
VEL5.3	5.3/4.38	1.0	10^{-9}	
VEL5.9	5.9/4.84	1.0	10^{-9}	
VEL6.4	6.4/5.29	1.0	10^{-9}	
VEL7.0	7.0/5.75	1.0	10^{-9}	
VEL7.5	7.5/6.2	1.0	10^{-9}	
PM0.1	4.8/3.93	0.1	10^{-9}	Sensitivity study on planet mass
PM0.3	4.8/3.93	0.3	10^{-9}	
PM0.5	4.8/3.93	0.5	10^{-9}	
PM0.7	4.8/3.93	0.7	10^{-9}	
PM2.0	4.8/3.93	2.0	10^{-9}	
PM3.0	4.8/3.93	3.0	10^{-9}	
DEN-7	4.8/3.93	1.0	10^{-7}	Sensitivity study on gas density
DEN-8	4.8/3.93	1.0	10^{-8}	
DEN-10	4.8/3.93	1.0	10^{-10}	

Orbit-dependent Simulation

Name	M_{pl} ($M_\oplus$)	a (au)	e	Comments
ORB	1.0	1.0	0.2	Time-dependent simulation to track orbital evolution

"Snapshot" simulations

- パラメータ：惑星と円盤ガスの相対速度・惑星質量・円盤ガス密度 (準)定常状態になるまで計算する。

Orbit-dependent simulation

- パラメータ： 惑星質量・軌道長半径・軌道離心率
- 他のパラメータは時間依存して変化する。
- 計算コストが高いため、1パラメータのみ計算する。

#42 Canonical case

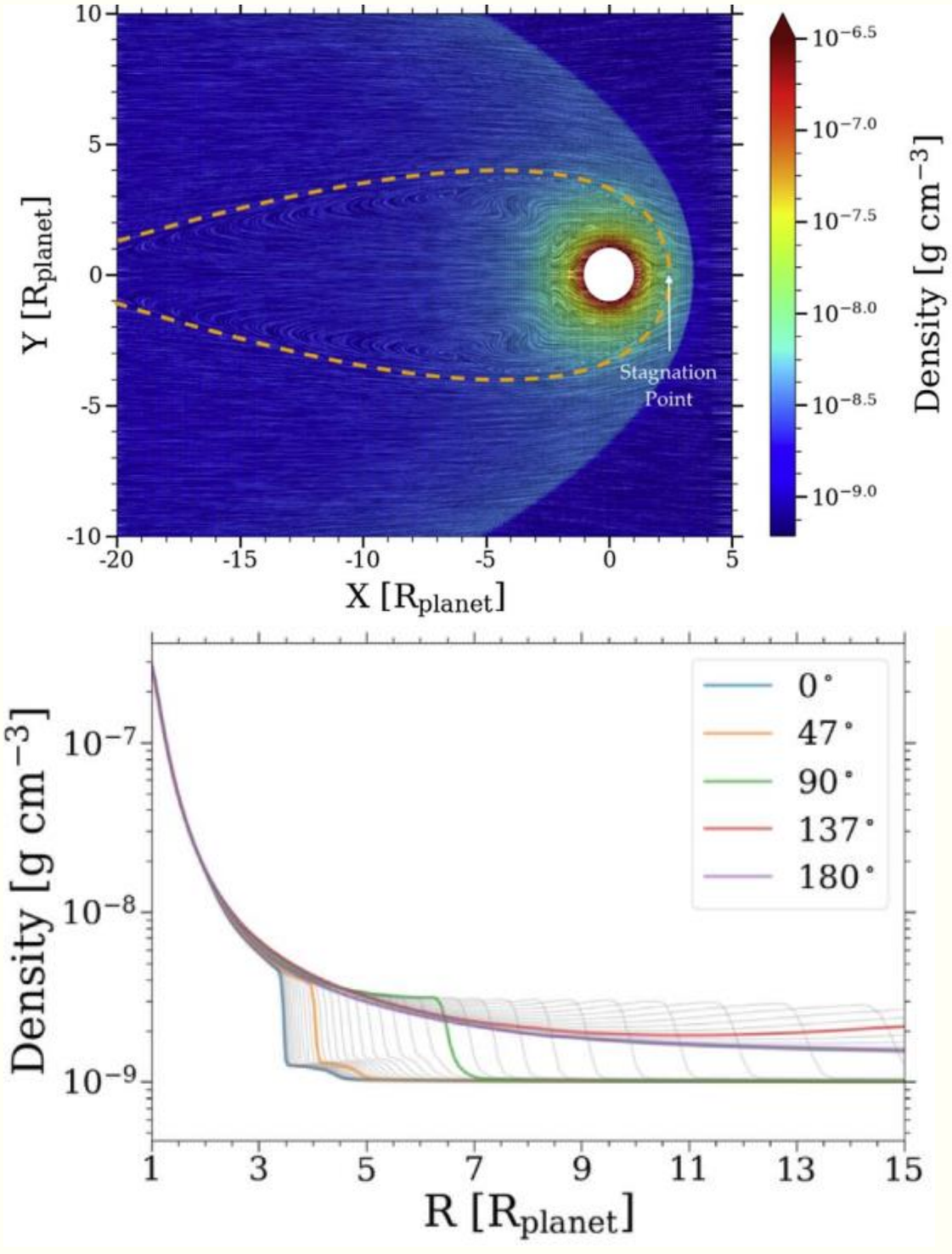

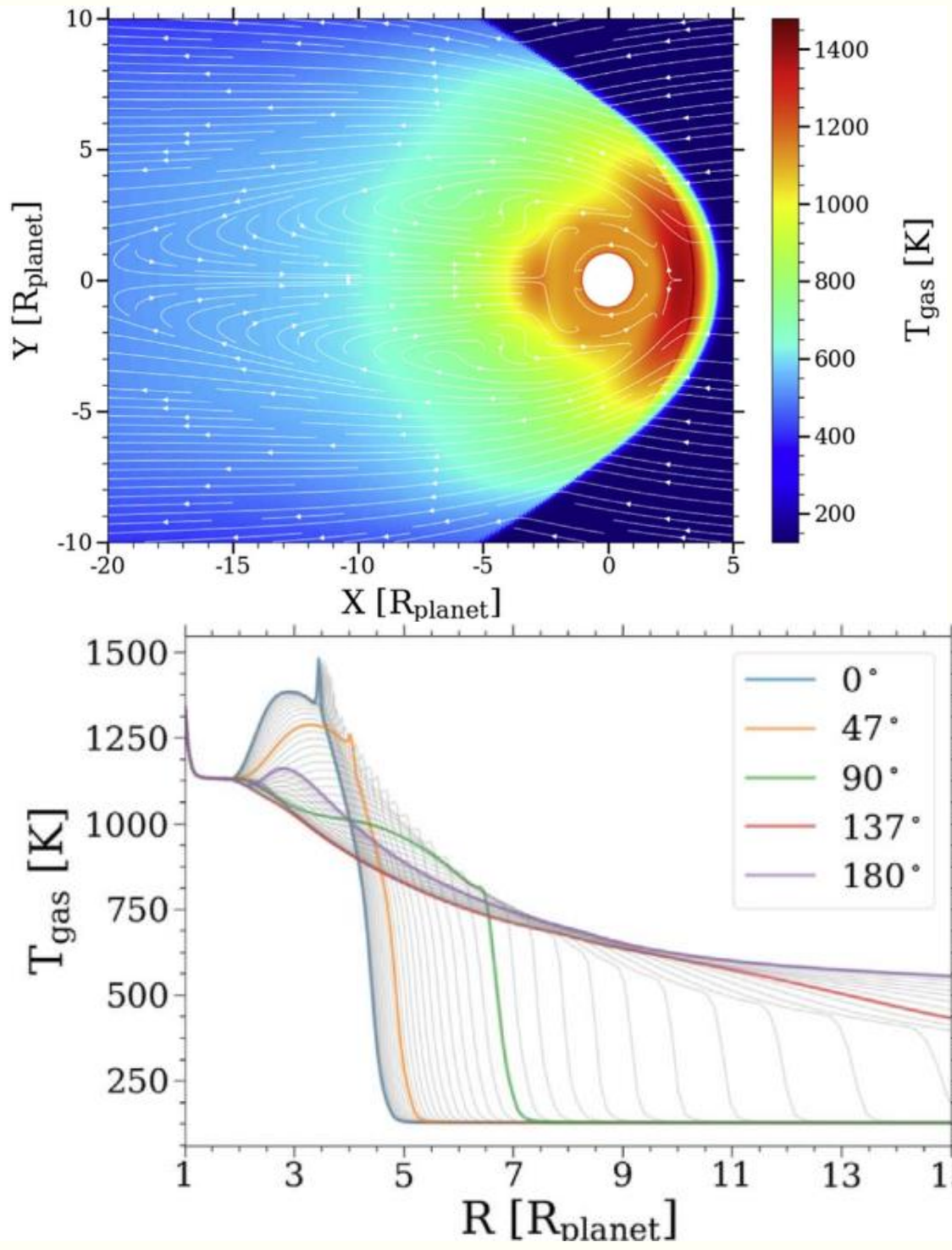

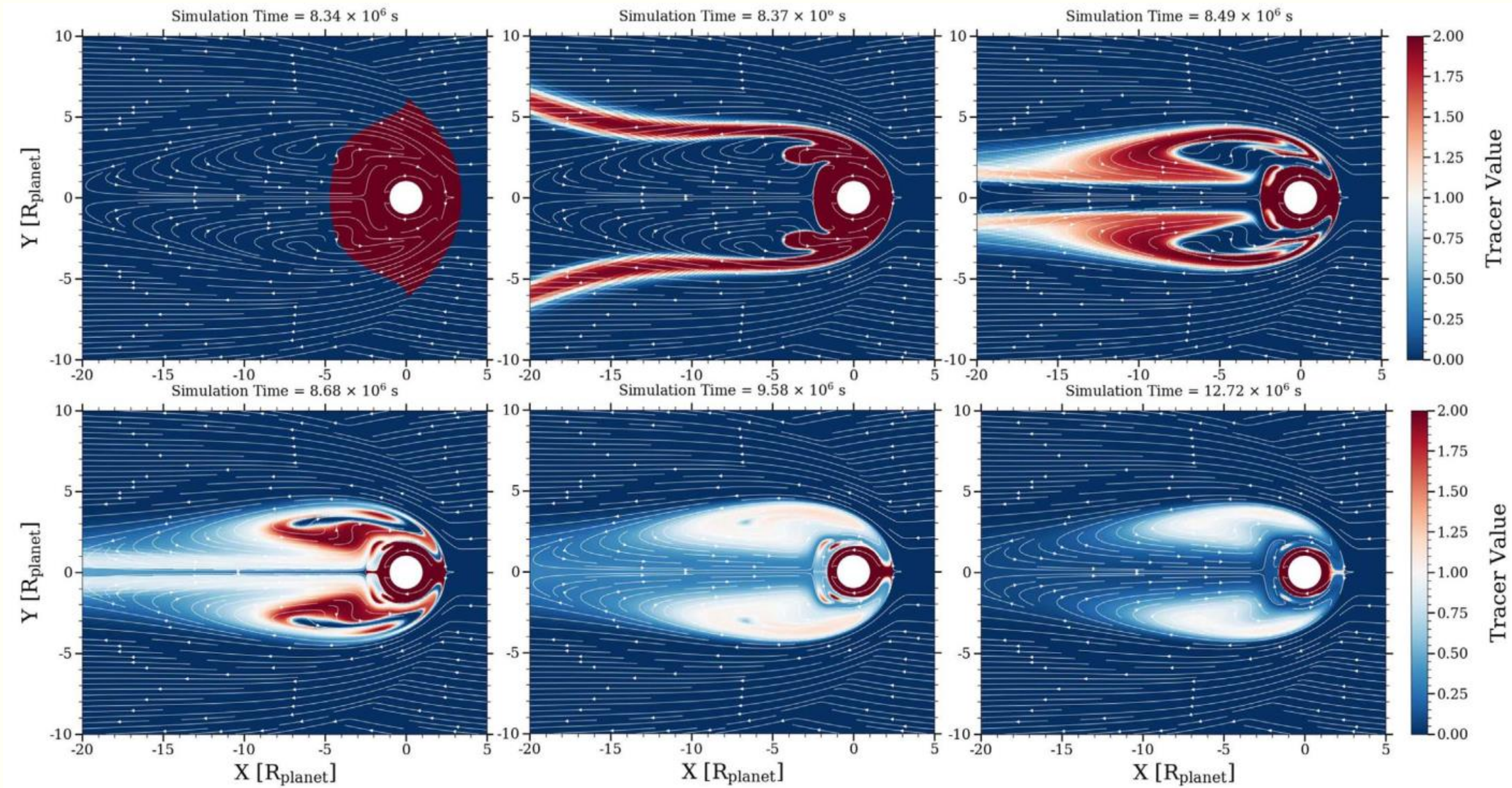

Figure 4. The movements of gas in the proto-atmosphere tracked with a tracer (initial value = 2) after the simulation reaches a quasi-steady state reveal the recycling of disk gas behind the planet. We set the initial dyed region to be the part of the atmosphere enclosed by the $10^{-8.5}$ g cm^{-3} density contour (one of the definitions of proto-atmospheres, see Section 3.1.2). The outermost layer of gas outside the "egg-shape" region directly flows out the computational domain, while the majority of gas circulates in vortices behind and around the planet. A portion of the gas stays bound around the planet, but the rest would flow out of the "egg-shape" region and be replaced by new incoming disk gas.

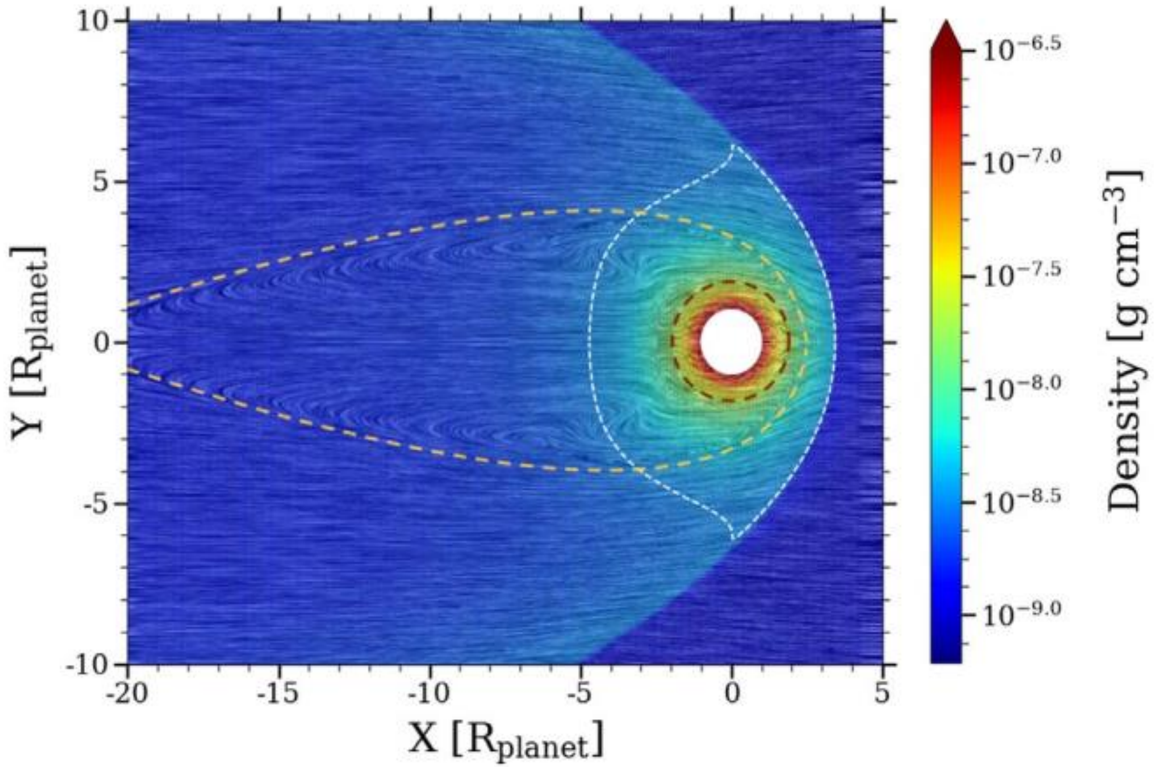

Figure 5. The three definitions of proto-atmospheres on eccentric planets. The white dashed line is the $10^{-8.5}$ g cm^{-3} density contour, the yellow dashed line denotes the boundary of the "egg-shape" region, and the red dashed line encloses the gas that is bound to the planet. The gas recycling region is between the red and yellow dashed lines.

原始大気の質量を計算するための定義

(A) **密度一定領域** ($10^{-8.5}$ g cm^{-3})

(B) ガスが入れ替わる**"egg-shape" region**

(C) 惑星による**重力束縛領域**

Canonical caseでの質量はそれぞれ

(A) 1.40e21 [g]

(B) 1.43e21 [g]

(C) 4.31e20 [g]

この定義によらない方法として、(D)**惑星表面における大気圧**を採用する。大気圧が大きいほど、多量の大気を持つ、と解釈する。

① 惑星と円盤ガスの相対速度

- v_∞ = 3.2 – 7.5 [km/s]
  ⇔ 軌道離心率 e = 0.1 – 0.5
- バウショックの強さを直接左右する。
- 相対速度が大きくなると、バウショックの開口角は小さくなる。
- 惑星が保持する原始大気も小さくなる。

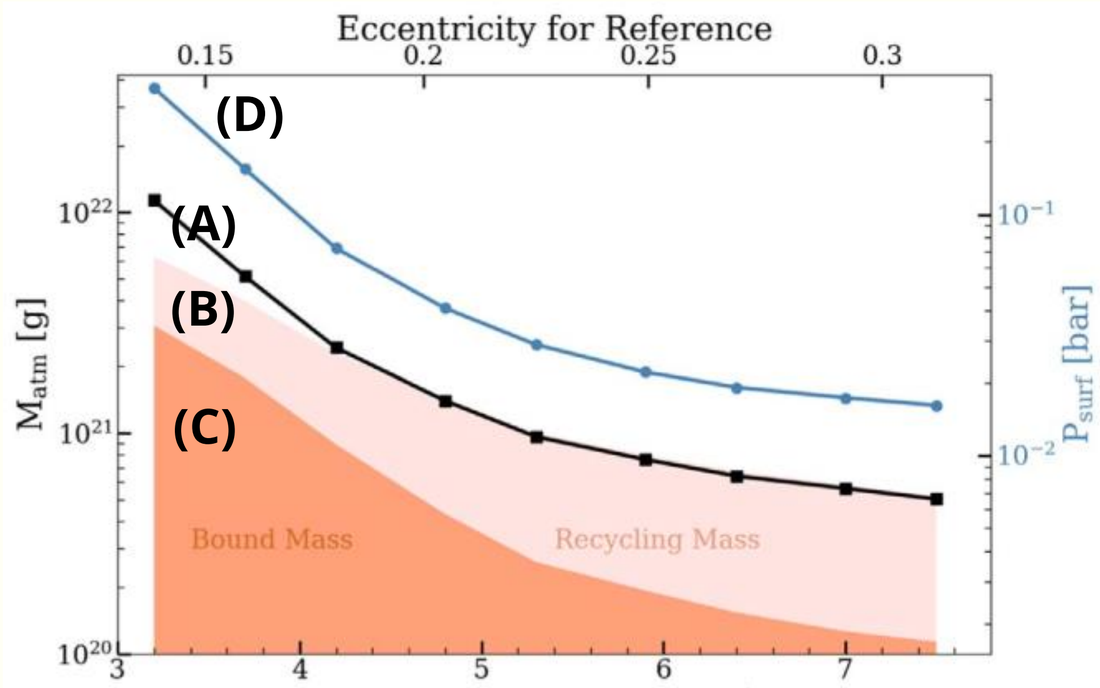

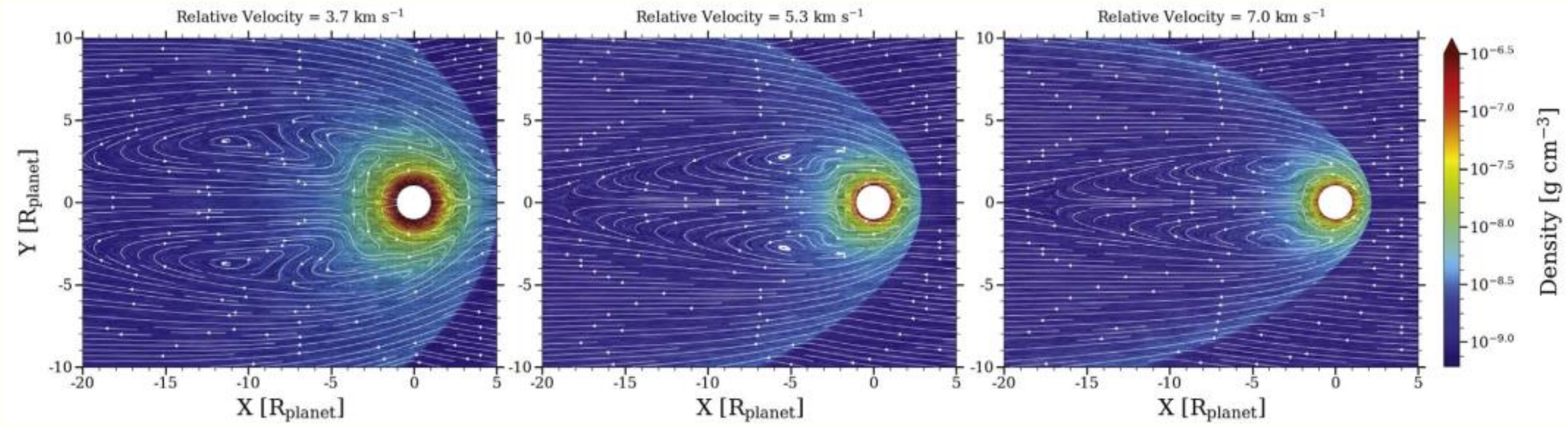

② 惑星質量

- M_{planet} = 0.1 – 3.0 [M_{earth}]
- 重力的に保持できる大気質量を決定する。
- M_{planet} = 0.1 [M_{earth}] (火星like)の場合のみ、通常の原始大気を保てなかった。バウショックが形成されず、流入ガスが直接惑星に衝突している。
- M_{planet} < 0.5 [M_{earth}]で入れ替わらない大気を保てなくなる。

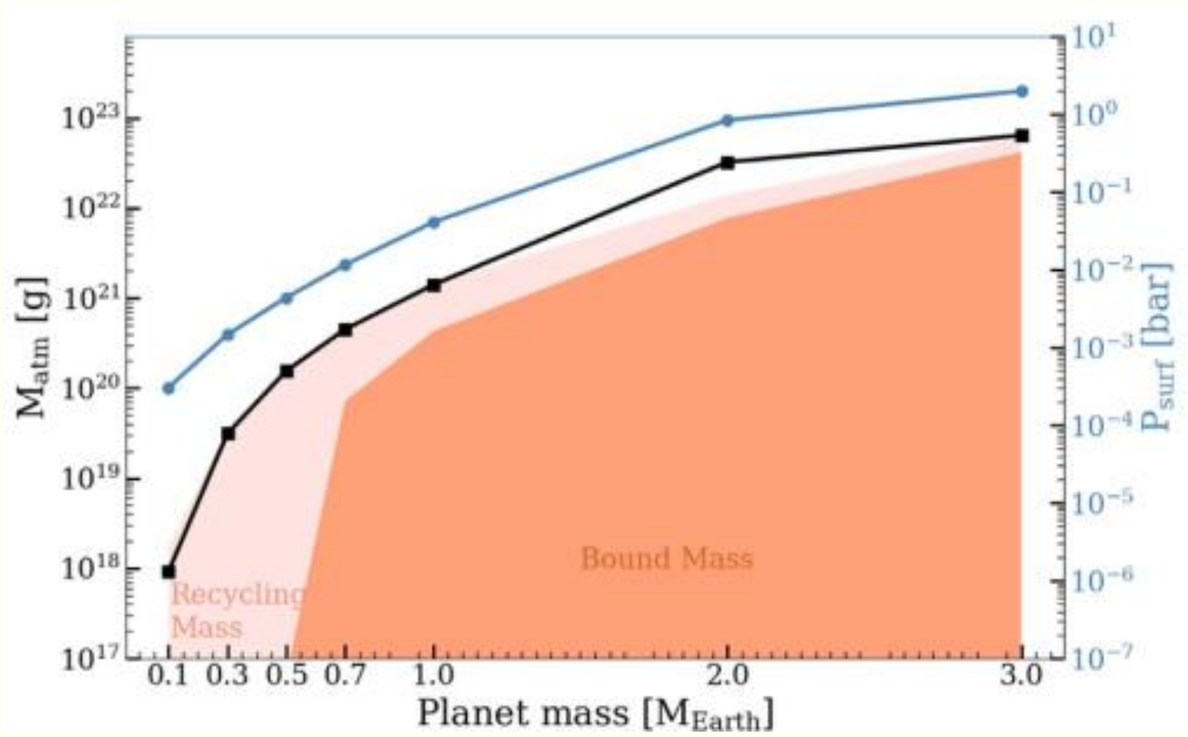

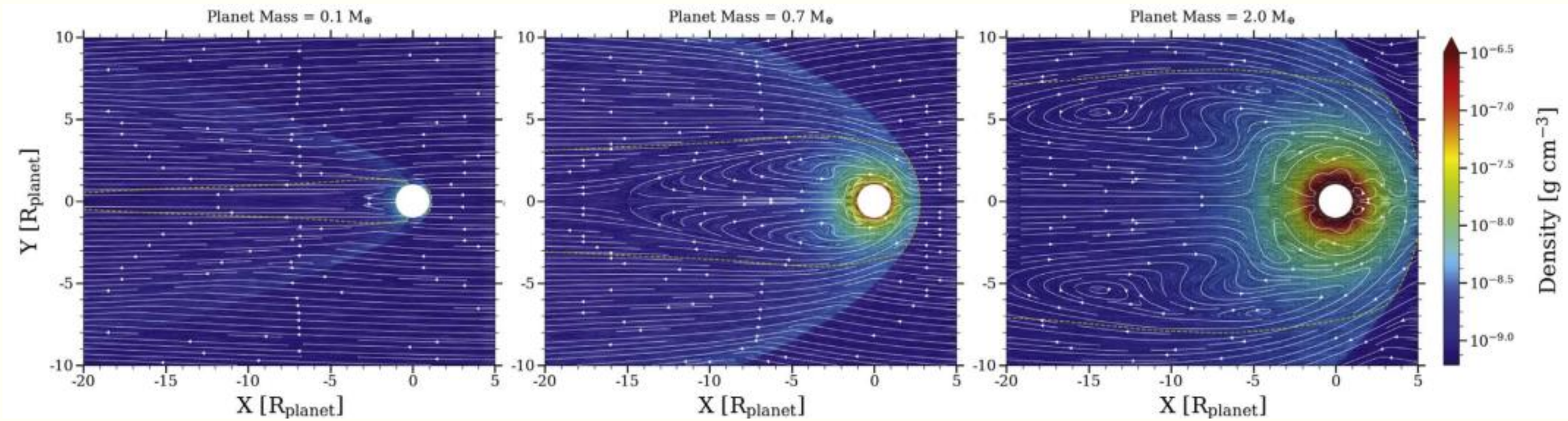

③ 円盤ガス密度

- $\rho_\infty = 10^{-10} – 10^{-7}$ [g cm^{-3}]
- 惑星が中心星に対して異なる距離にいる場合に対応する。
- 他のパラメータに比べて明快ではない。
- 密度を下げると、ガス圧・ラム圧が低下し、バウショックが弱まることでより多くの大気が惑星に降着する。
- 密度を上げると、リサイクル領域(egg-shape region)がなくなる。
- 高密度では、流入ガス量の増加によって大気質量も増加する。

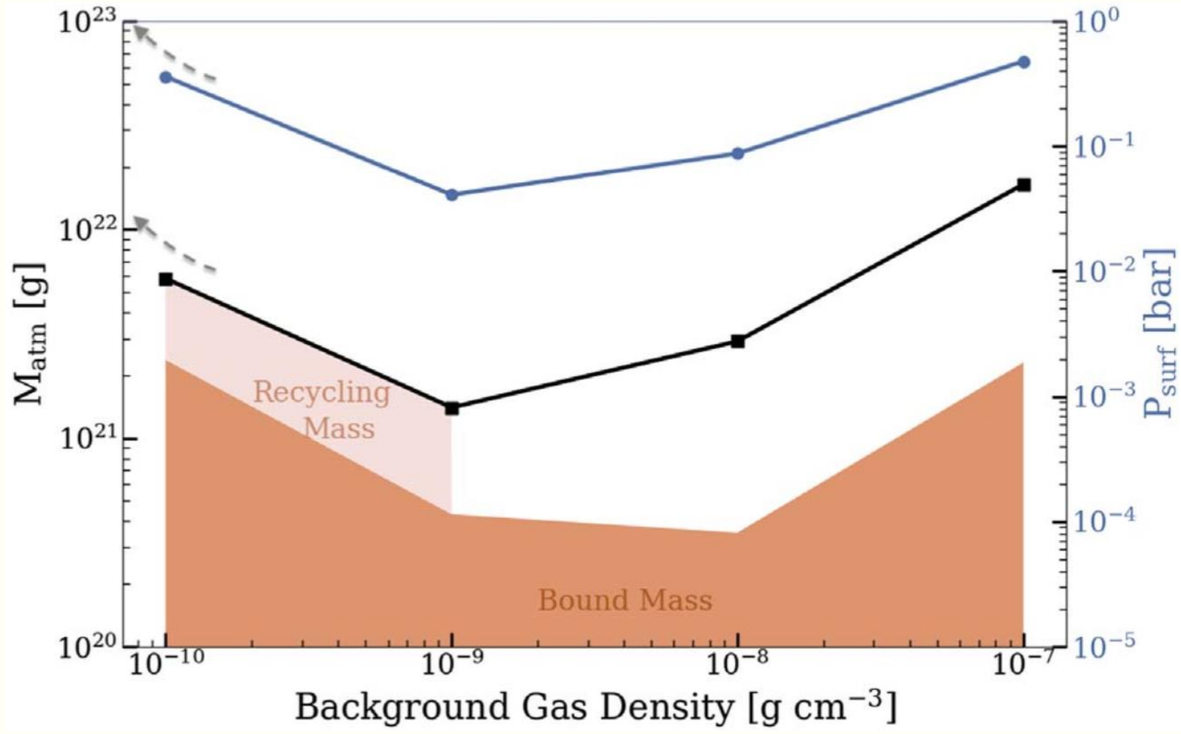

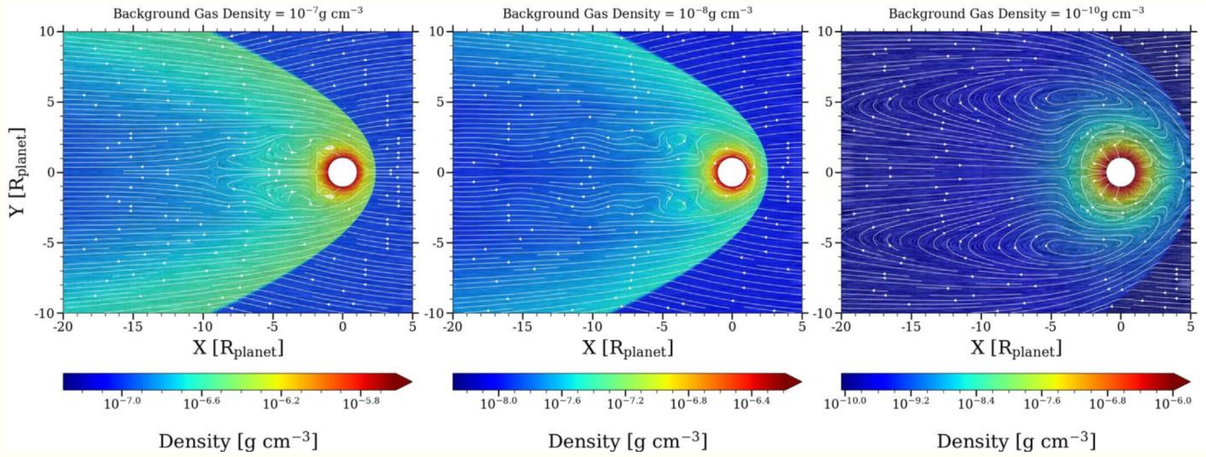

#42 Orbit-dependent simulation (time-evolution)

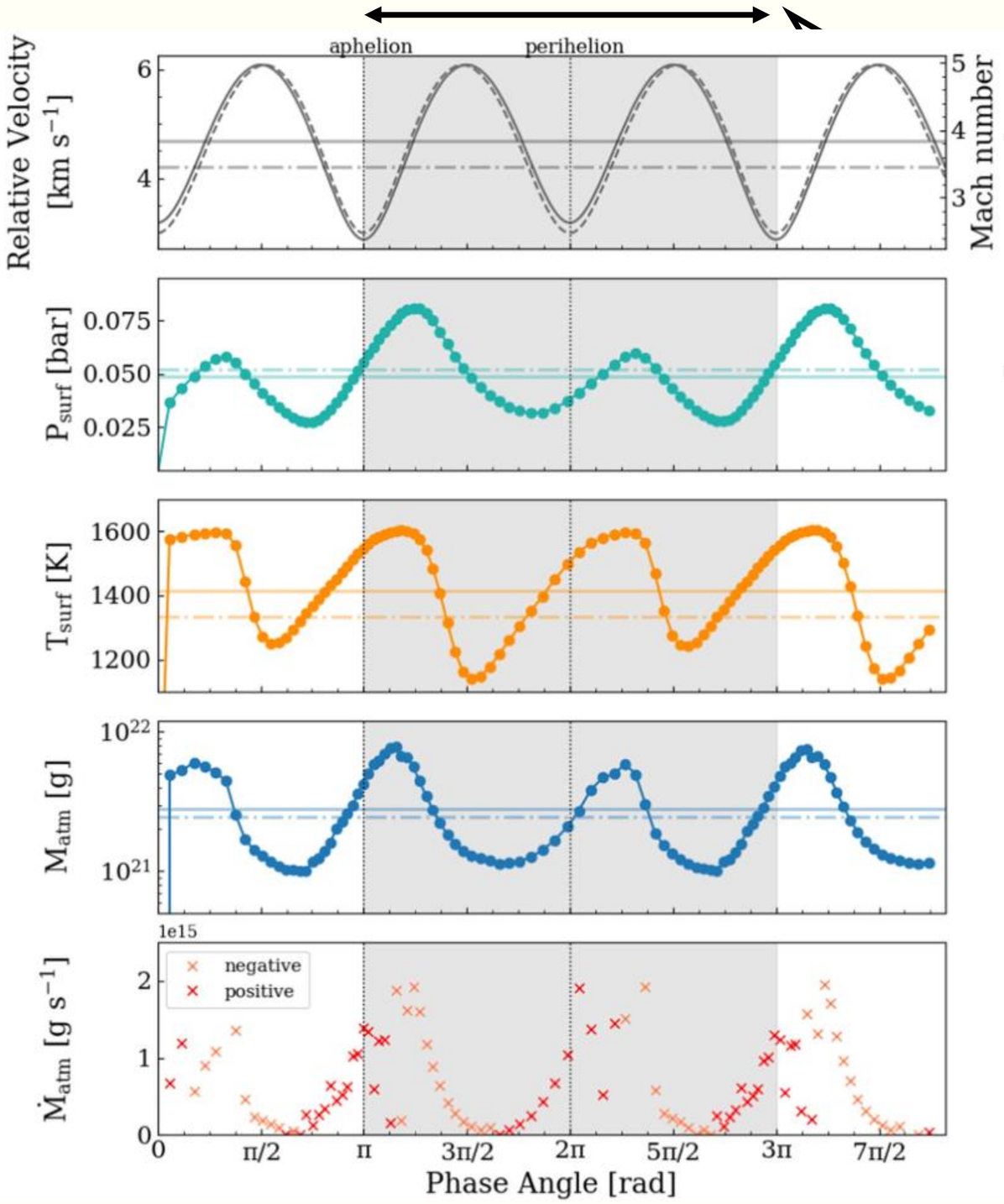

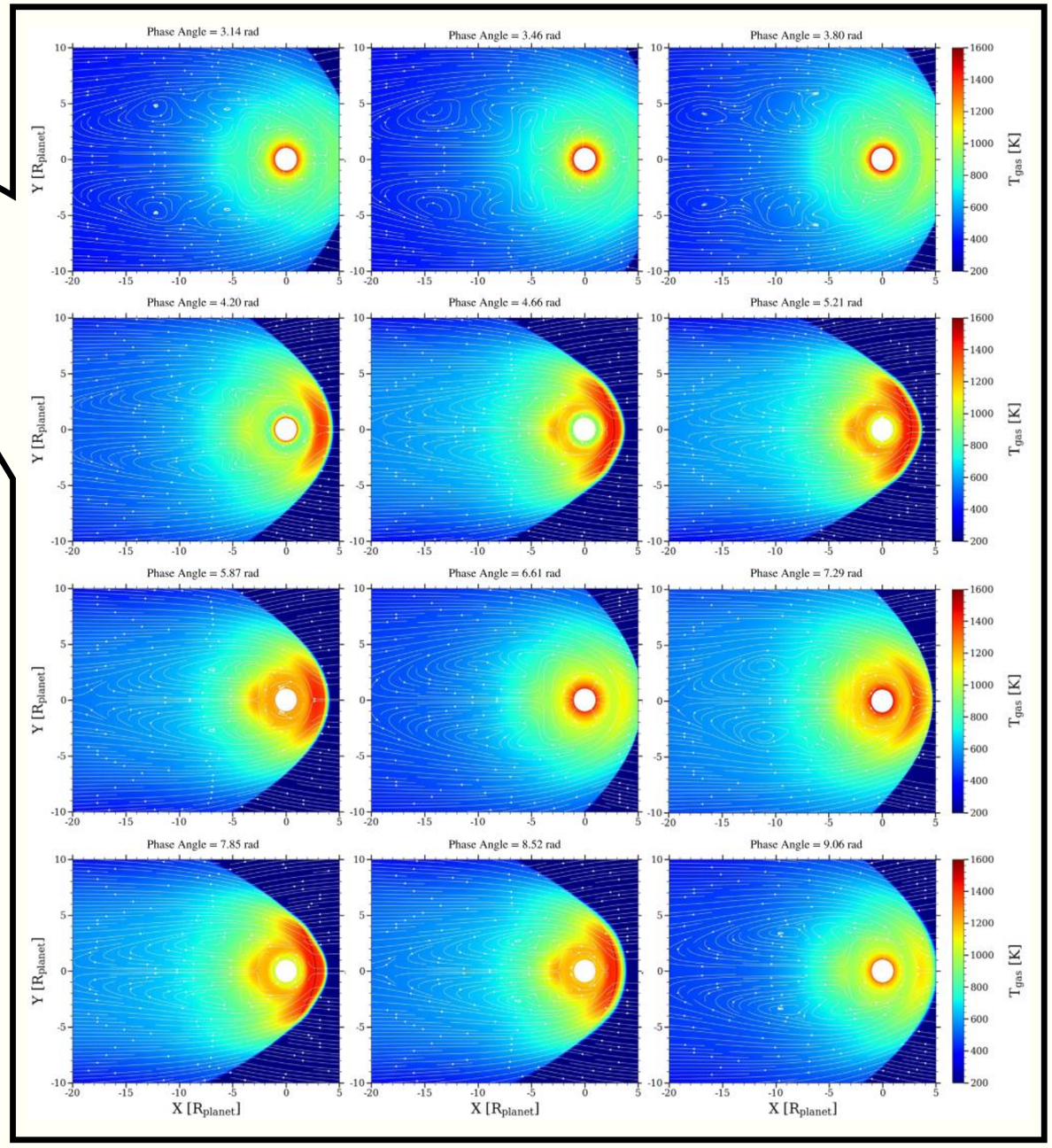

- 流体シミュレーションは定常状態に達する。

- バウショックに流入したガスは、”egg-shape”領域を形成する。この領域内で、原始大気は周辺領域とガスを交換する。惑星近傍には小さな重力束縛大気が、交換されず保たれる。
- 円軌道惑星に比べて、偏心惑星の原始大気は3–4桁小さな質量しか持たない。惑星のmigration・散乱は原始大気を大きく減らす (mass lossの原因となる)。

- パラメータ依存性
  - 相対速度 **増** ➔ 原始大気 **減**
  - 惑星質量 **増** ➔ 原始大気 **増**
  - 背景密度 **増** ➔ 原始大気 **減→増**

- 原始大気の物理量は、惑星の軌道運動に応じて振動する。
- 平均的な描像は、snapshot simulation (定常状態) で再現できる。

Implementation of stellar heating feedback in simulations of star cluster formation: effects on the initial mass function

Show affiliations

Mathew, Sajay Sunny; Federrath, Christoph

Explaining the initial mass function (IMF) of stars is a long-standing problem in astrophysics. The number of complex mechanisms involved in the process of star cluster formation, such as turbulence, magnetic fields, and stellar feedback, make understanding and modelling the IMF a challenging task. In this paper, we aim to assert the importance of stellar heating feedback in the star cluster formation process and its effect on the shape of the IMF. We use an analytical sub-grid model to implement the radiative feedback in fully three-dimensional magnetohydrodynamical (MHD) simulations of star cluster formation, with the ultimate objective of obtaining numerical convergence on the IMF. We compare a set of MHD adaptive mesh refinement simulations with three different implementations of the heating of the gas: (1) a polytropic equation of state, (2) a spherically symmetric stellar heating feedback, and (3) our newly developed polar heating model that takes into account the geometry of the accretion disc and the resulting shielding of stellar radiation by dust. For each of the three heating models, we analyse the distribution of stellar masses formed in 10 molecular cloud simulations with different realizations of the turbulence to obtain a statistically representative IMF. We conclude that stellar heating feedback has a profound influence on the number of stars formed and plays a crucial role in controlling the IMF. We find that the simulations with the polar heating model achieve the best convergence on the observed IMF.

https://ui.adsabs.harvard.edu/abs/2020MNRAS.496.5201M/abstract

星団形成3D-MHDシミュレーションに、星からの過熱フィードバックをsub-gridモデルとして実装。3通りのモデルを試す。

降着円盤による輻射フィードバックへの遮蔽効果を考慮したモデルが、観測されているIMFを最もよく再現する。

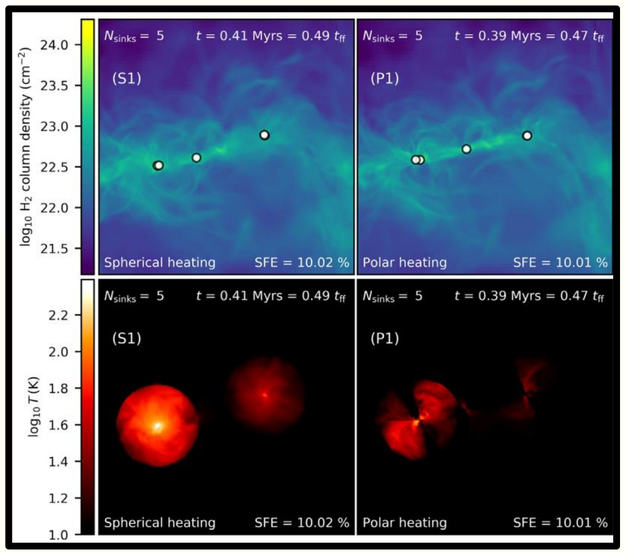

Ejection of close-in super-Earths around low-mass stars in the giant impact stage

Hide affiliations

Matsumoto, Yuji (-); Gu, Pin-Gao (-); Kokubo, Eiichiro (-); Oshino, Shoichi (-); Omiya, Masashi (-)

Earth-sized planets were observed in close-in orbits around M dwarfs. While more and more planets are expected to be uncovered around M dwarfs, theories of their formation and dynamical evolution are still in their infancy. We investigate the giant impact growth of protoplanets, which includes strong scattering around low-mass stars. The aim is to clarify whether strong scattering around low-mass stars affects the orbital and mass distributions of the planets. We perform N-body simulation of protoplanets by systematically surveying the parameter space of the stellar mass and surface density of protoplanets. We find that protoplanets are often ejected after twice or three times close-scattering around late M dwarfs. The ejection sets the upper limit of the largest planet mass. Adopting the surface density scaling linearly with the stellar mass, we find that as the stellar mass decreases less massive planets are formed in orbits with higher eccentricities and inclinations. Under this scaling, we also find that a few close-in protoplanets are generally ejected. The ejection of protoplanets plays an important role in the mass distribution of super-Earths around late M dwarfs. The mass relation of observed close-in super-Earths and their central star mass is well reproduced by ejection.

https://ui.adsabs.harvard.edu/abs/2020arXiv200714039M/abstract

ジャイアントインパクトによる原始惑星の軌道・質量分布への影響を調べる。

原始惑星のN体シミュレーション

原始惑星は2-3回の近接散乱の後に惑星系からよく放出される。**中心星質量が小さいほど、より低質量の惑星が大きな軌道離心率と傾きを持つ軌道に形成**される。

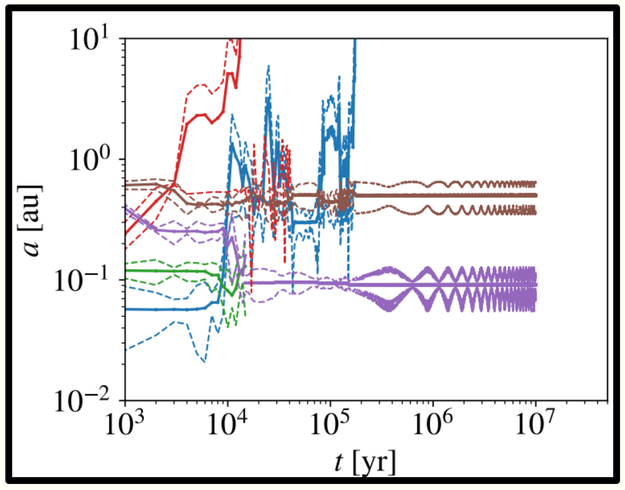

Magnetohydrodynamic Accretion-Ejection: Jets Launched by a Nonisotropic Accretion-disk Dynamo. I. Validation and Application of Selected Dynamo Tensorial Components

Show affiliations

Mattia, Giancarlo; Fendt, Christian

Astrophysical jets are launched from strongly magnetized systems that host an accretion disk surrounding a central object. The origin of the jet-launching magnetic field is one of the open questions for modeling the accretion-ejection process. Here we address the question of how the accretion-disk magnetization and field structure required for jet launching are generated. Applying the PLUTO code, we present the first resistive magnetohydronamic simulations of jet launching including a nonscalar accretion-disk mean-field $\alpha^2\Omega$ dynamo in the context of large-scale disk-jet simulations. Essentially, we find the α_φ-dynamo component determining the amplification of the poloidal magnetic field, which is strictly related to the disk magnetization (and, as a consequence, to the jet speed, mass, and collimation), while the α_R- and α_θ-dynamo components trigger the formation of multiple, antialigned magnetic loops in the disk, with strong consequences for the stability and dynamics of the disk-jet system. In particular, such loops trigger the formation of dynamo-inefficient zones, which are characterized by a weak magnetic field and therefore a lower value of the magnetic diffusivity. The jet mass, speed, and collimation are strongly affected by the formation of the dynamo-inefficient zones. Moreover, the θ component of the α dynamo plays a key role when the dynamo interacts with a nonradial component of the seed magnetic field. We also present correlations between the strength of the disk toy dynamo coefficients and the dynamical parameters of the jet that is launched.

https://ui.adsabs.harvard.edu/abs/2020ApJ...900...59M/abstract

ジェット駆動に必要な降着円盤磁化と磁場構造はどのように作られるのか

非スカラー降着円盤平均場ダイナモを初めて取り入れたジェット駆動の非理想磁気流体シミュレーション

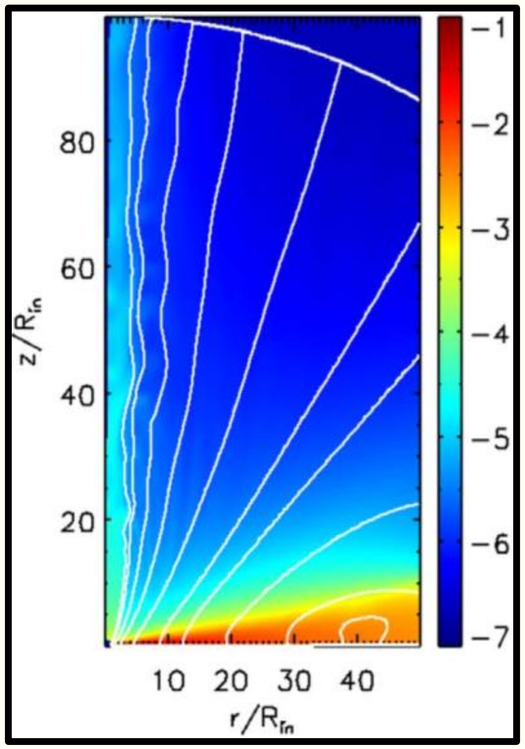

Magnetohydrodynamic Accretion-Ejection: Jets Launched by a Nonisotropic Accretion-disk Dynamo. II. A Dynamo Tensor Defined by the Disk Coriolis Number

Show affiliations

Mattia, Giancarlo; Fendt, Christian

Astrophysical jets are launched from strongly magnetized systems that host an accretion disk surrounding a central object. Here we address the question of how accretion-disk magnetization and the field structure required for jet launching are generated. We continue our work from Mattia & Fendt (Paper I) by considering a nonscalar accretion-disk mean-field &agr;$^2\Omega$ dynamo in the context of large-scale disk-jet simulations. We now investigate a disk dynamo that follows analytical solutions of the mean-field dynamo theory, essentially based only on a single parameter, the Coriolis number. We thereby confirm the anisotropy of the dynamo tensor acting in accretion disks, allowing both the resistivity and mean-field dynamo to be related to the disk turbulence. Our new model recovers previous simulations by applying a purely radial initial field while allowing for a more stable evolution for seed fields with a vertical component. We also present correlations between the strength of the disk dynamo coefficients and the dynamical parameters of the jet that is launched, and discuss their implications for observed jet quantities.

(Paper Iの続き)

平均場ダイナモ理論の解析解に従う円盤ダイナモを調べた

新モデルによって以前のシミュレーション結果を再現できる。

https://ui.adsabs.harvard.edu/abs/2020ApJ...900...60M/abstract

The magnetic obliquity of accreting T Tauri stars

Show affiliations

McGinnis, Pauline; Bouvier, Jérôme; Gallet, Florian

Classical T Tauri stars (CTTSs) accrete material from their discs through their magnetospheres. The geometry of the accretion flow strongly depends on the magnetic obliquity, i.e. the angle between the rotational and magnetic axes. We aim at deriving the distribution of magnetic obliquities in a sample of 10 CTTSs. For this, we monitored the radial velocity variations of the He I λ5876 Å line in these stars' spectra along their rotational cycle. He I is produced in the accretion shock, close to the magnetic pole. When the magnetic and rotational axes are not aligned, the radial velocity of this line is modulated by stellar rotation. The amplitude of modulation is related to the star's projected rotational velocity, vsin i, and the latitude of the hotspot. By deriving vsin i and He I λ5876 radial velocity curves from our spectra, we thus obtain an estimate of the magnetic obliquities. We find an average obliquity in our sample of 11.4° with an rms dispersion of 5.4°. The magnetic axis thus seems nearly, but not exactly aligned with the rotational axis in these accreting T Tauri stars, somewhat in disagreement with studies of spectropolarimetry, which have found a significant misalignment (≳20°) for several CTTSs. This could simply be an effect of low number statistics, or it may be due to a selection bias of our sample. We discuss possible biases that our sample may be subject to. We also find tentative evidence that the magnetic obliquity may vary according to the stellar interior and that there may be a significant difference between fully convective and partly radiative stars.

古典的Tタウリ星への降着流の形状は、**回転軸と磁力線方向の角度(=磁気傾斜)**に依存する。

古典的Tタウリ星10サンプルの磁気傾斜分布を観測より求めた。

平均 θ = 11.4°±5.4°

これは他の測定値(>20°)に比べて小さい。

https://ui.adsabs.harvard.edu/abs/2020MNRAS.497.2142M/abstract